

# EFFECTS OF SHEAR AND ROTATION ON TURBULENT FLOW IN A STRATIFIED FLUID

Frank G. Jacobitz  
Mechanical Engineering Program  
University of San Diego  
5998 Alcalá Park  
San Diego, California 92110, USA  
Jacobitz@SanDiego.Edu

## ABSTRACT

The effect of rotation on the evolution of turbulence in a stably stratified shear flow is studied using direct numerical simulations. The prototypical example of this flow is considered here with uniform vertical shear, constant system rotation about the vertical axis, and uniform vertical stable density stratification. In the absence of rotation, growth of the turbulent kinetic energy is observed for weakly stratified flows. As the stratification is increased, the growth of the turbulent kinetic energy weakens and decay is observed for strongly stratified flows. Counter-gradient fluxes are observed in the strongly stratified cases. For moderate stratification, rotation leads to a stronger growth of the turbulent kinetic energy. For strong stratification, however, virtually no effect of rotation on the evolution of the turbulent kinetic energy was observed for the range of parameters studied here. The tendency for counter-gradient fluxes was observed to decrease with increasing rotation for strongly stratified flow.

## INTRODUCTION

Direct numerical simulations are performed in order to study the effects of mean velocity shear and system rotation on turbulent flow in a stably stratified fluid. The flow considered here has uniform vertical shear, constant system rotation about the vertical axis, and uniform vertical stable stratification. A schematic of this flow is shown in figure 1. In this flow, the mean downstream velocity component and the mean density vary linearly in the vertical direction:

$$U = Sz \quad V = W = 0 \quad \varrho = \rho_0 + S_\rho z \quad (1)$$

The shear rate  $S = \partial U / \partial z$ , the Coriolis parameter  $f = 2\Omega$ , and the stratification rate  $S_\rho = \partial \varrho / \partial z$  are constant.

Due to its geophysical importance (see for example Caldwell and Moum, 1995), turbulence in a stably stratified fluid has been studied extensively in the past, both experimentally (Itsweire, Helland, and Van Atta, 1986; Yoon and Warhaft, 1990; Komori and Nagata, 1996) and numerically (Riley, Metcalfe and Weissman, 1981; Métais and Herring, 1989; Kimura and Herring, 1996). Similarly, extensive work has been performed to understand turbulent stratified shear flows. Using energy considerations, Richardson (1920) and Taylor (1931) established the Richardson number  $Ri = N^2/S^2$  as the primary parameter to describe the stability of stratified shear flow. Here,  $N = \sqrt{-gS_\rho/\rho_0}$  is the Brunt-Väisälä frequency and  $S$  is the shear rate. Miles (1961) and Howard (1961)

showed that the flow is stable for  $Ri > 1/4$  using linear inviscid stability analysis. More recently, stably stratified shear flow has been studied in great detail, both experimentally (Komori, Ueda, Ogino, and Mizushima, 1983; Rohr, Itsweire, Helland, and Van Atta, 1988; Piccirillo and Van Atta, 1997), as well as numerically (Gerz, Schumann, and Elghobashi, 1989; Holt, Koseff, and Ferziger, 1992; Itsweire, Koseff, Briggs, and Ferziger, 1993; Jacobitz, Sarkar, and Van Atta, 1997; Jacobitz, 2000). Rotating stratified turbulence has received less attention (Bartello, 1995; Iida and Nagano, 1999). Winters and MacKinnon (2004) show that instability can exist in a rotating stably stratified shear flow for Richardson numbers  $Ri > 1/4$  using linear inviscid stability theory. Rapid distortion results for these flows were obtained by Hanazaki and Hunt (1996) for stably stratified flow, Hanazaki (2002) for unstably stratified flow, and Hanazaki and Hunt (2004) for stably stratified shear flow.

The goal of this work is to help understand the evolution of turbulence in a stratified fluid in the presence of shear and rotation. In the following sections, the numerical approach is introduced, results from simulations with and without system rotation are discussed, and the results are summarized.

## NUMERICAL APPROACH

In this study the prototypical flow with uniform shear  $S = \partial U / \partial z$ , system rotation about the vertical axis with constant Coriolis parameter  $f = 2\Omega$ , and uniform stable stratification  $S_\rho = \partial \rho / \partial z$  is considered. Both the shear rate  $S$  and the stratification rate  $S_\rho$  remain constant as the simulations are advanced in time. A geostrophic balance for the mean velocity field and a hydrostatic balance for the mean density field are assumed.

The direct numerical simulations are based on the continuity equation for an incompressible fluid, the unsteady three-dimensional Navier-Stokes equation in the Boussinesq approximation, and an advection-diffusion equation for the density. In the direct numerical approach, all dynamically important scales of the velocity and density fields are resolved. The equations are solved in a frame of reference moving with the mean flow (Rogallo, 1981). This approach allows the use of periodic boundary conditions for the fluctuating components of the velocity and density fields. A spectral collocation method is used for the spatial discretization and the solution is advanced in time with a fourth-order Runge-Kutta scheme. The simulations are performed on a parallel computer using a grid with up to  $256 \times 256 \times 256$  points.

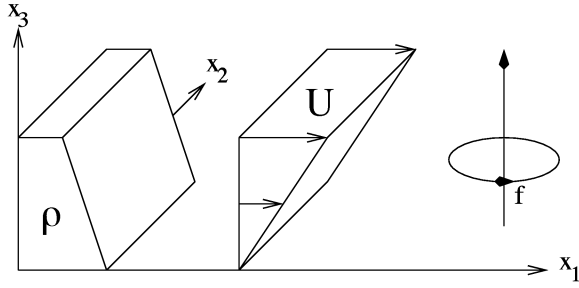


Figure 1: Schematic of the flow considered here.

## RESULTS

In the following, the results from three series of simulations are presented. In the first series, non-rotating stratified shear flow is considered and the Richardson number is varied from  $Ri = 0$ , corresponding to unstratified shear flow, to  $Ri = 1$ , corresponding to strongly stratified shear flow. In the second and third series of simulations, the Richardson number is fixed to a value  $Ri = 0.2$  and  $Ri = 1$ , respectively, and the strength of the rotation is varied from  $f/S = 0$ , corresponding to no rotation, to  $f/S = 2$ , corresponding to strong rotation. All simulations are initialized with isotropic turbulence fields without density fluctuations. The initial Taylor microscale Reynolds number  $Re_\lambda = 35$  and the initial shear number  $SK/\epsilon = 2$  are matched in all cases. The Reynolds number reaches values as high as  $Re_\lambda = 100$  and the shear number assumes a value  $SK/\epsilon = 6$  in the simulations. The molecular Prandtl number of the density field is  $Pr = 0.7$ .

### Non-rotating Stratified Shear Flow

In this section, results from a series of simulations of non-rotating stably stratified shear flow are presented. The Richardson number is varied from  $Ri = 0$  to  $Ri = 1$ . Figure 2 shows the evolution of the turbulent kinetic energy  $K = \overline{u_i u_i} / 2$  with non-dimensional time  $St$ . Initially, the turbulent kinetic energy decays due to the isotropic initial conditions until the shear production of turbulence develops at about  $St = 2$ . For strongly stratified cases with Richardson numbers  $Ri > 0.1$ , the turbulent kinetic energy continues to decay. For cases with  $Ri < 0.1$ , the turbulent kinetic energy eventually grows as the simulations advance. Note that the value of the critical Richardson number observed here is somewhat smaller than the value of one quarter determined from linear inviscid stability theory by Miles (1961) and Howard (1961).

The transport equation for the turbulent kinetic energy equation can be written in the following non-dimensional form:

$$\frac{1}{SK} \frac{dK}{dt} = \frac{P}{SK} - \frac{B}{SK} - \frac{\epsilon}{SK}$$

Here  $P = -S\overline{uw}$  is the production rate,  $B = g\overline{w\rho}/\rho_0$  is the buoyancy flux, and  $\epsilon$  is the viscous dissipation rate. Figure 3 shows the evolution of the normalized production rate  $P/SK$ , buoyancy flux  $B/SK$ , and dissipation rate  $\epsilon/SK$  for two simulations with  $Ri = 0.1$  (solid lines) and  $Ri = 0.5$  (dashed lines). As the Richardson number is increased, the normalized production rate  $P/SK$  and the normalized buoyancy flux  $B/SK$  decrease strongly, resulting in decay of the turbulent kinetic energy. In the weakly stratified case with  $Ri = 0.1$ , both  $P/SK$  and  $B/SK$  are positive, indicating down-gradient

fluxes. Both  $P/SK$  and  $B/SK$  are negative in the strongly stratified case with  $Ri = 0.5$  and the fluxes are counter-gradient. The fluctuations of  $P/SK$  and  $B/SK$  point to the presence of internal waves in the  $Ri = 0.5$  case. A more extensive discussion of the energetics of stably stratified shear flow can be found in Jacobitz *et al.* (1997).

Figure 4 shows the evolution of the eddy viscosity  $\nu_t = -\overline{uw}/S$  as computed from the direct numerical data. As the Richardson number is increased, the eddy viscosity decreases, indicating a strong suppression of turbulent mixing with increasing density stratification.

Figure 5 shows the final values of the components of the shear stress anisotropy tensor  $b_{ij}$  at non-dimensional time  $St = 10$ . The diagonal components (full symbols) describe the distribution of the turbulent kinetic energy. As shear production adds energy to the downstream component and buoyancy extracts energy from the vertical component, the components are ordered  $b_{11} > b_{22} > b_{33}$  or downstream  $>$  spanwise  $>$  vertical. The magnitude of the off-diagonal component  $b_{13}$  is a measure of turbulence production. For strongly stratified cases, it switches sign, indicating a counter-gradient transport (Komori *et al.*, 1983). The maximum anisotropy is found for the cases in which  $b_{13}$  has changed sign in agreement with Holt *et al.* (1992).

### Rotating Stratified Shear Flow

This section compares the effect of rotation on the evolution of turbulence in a stably stratified shear flow at the two Richardson numbers  $Ri = 0.2$  and  $Ri = 0.5$ . The initial conditions are identical to the non-rotating cases discussed in the previous section.

#### Moderate Stratification with $Ri = 0.2$ .

Figure 6 shows the evolution of the turbulent kinetic energy  $K$  for a series of simulations in which the ratio  $f/S$  is varied from  $f/S = 0$ , corresponding to non-rotating flow, to  $f/S = 2$ , corresponding to strongly rotating flow. The Richardson number  $Ri = 0.2$  is fixed in these cases. The case with no rotation ( $f/S = 0$ ) shows decay of the turbulent kinetic energy. The weakly rotating cases with  $f/S = 0.1$  and  $f/S = 0.2$  show a higher level of the turbulent kinetic energy, but  $K$  continues to decay. The strongly rotating cases with  $f/S = 0.5$ ,  $f/S = 1$ , and  $f/S = 2$  show eventual growth of the turbulent kinetic energy  $K$ . Initially, an increasing ratio  $f/S$  leads to a stronger decay of the turbulent kinetic energy  $K$ . Also, independent of the ratio  $f/S$ , a non-dimensional time  $St = 7$  is required for growth of  $K$  to be obtained in the strongly rotating simulations. This compares to a non-dimensional time of  $St = 2$  for shear production of turbulence to result in growth of  $K$  in weakly stratified non-rotating cases.

Figure 7 shows the evolution of the normalized production rate  $P/SK$ , buoyancy flux  $B/SK$ , and dissipation rate  $\epsilon/SK$  for two simulations with  $f/S = 0.1$  (solid lines) and  $f/S = 1$  (dashed lines). Rotation affects the normalized dissipation rate  $\epsilon/SK$  only slightly, but strongly increases both the normalized production rate  $P/SK$  and the normalized buoyancy flux  $B/SK$ . Note that in the strongly rotating cases  $P/SK$  and  $B/SK$  do not reach statistically steady values as observed in the non-rotating cases, but rather increase to the end of the simulations.

The evolution of the eddy viscosity  $\nu_t$  is presented in figure

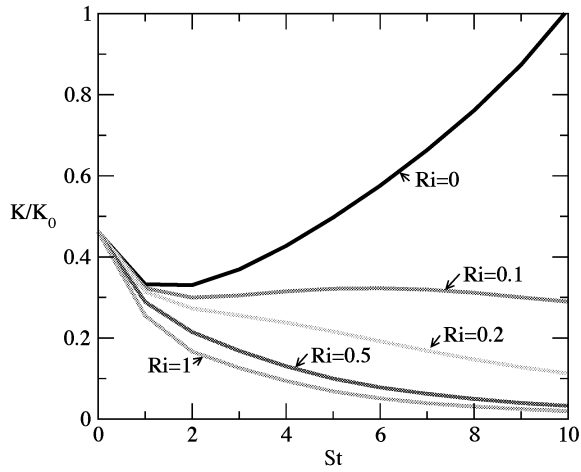


Figure 2: Evolution of the turbulent kinetic energy for a series of simulations in which the Richardson number is varied from  $Ri = 0$  to  $Ri = 1$ . There is no rotation and  $f/S = 0$ .

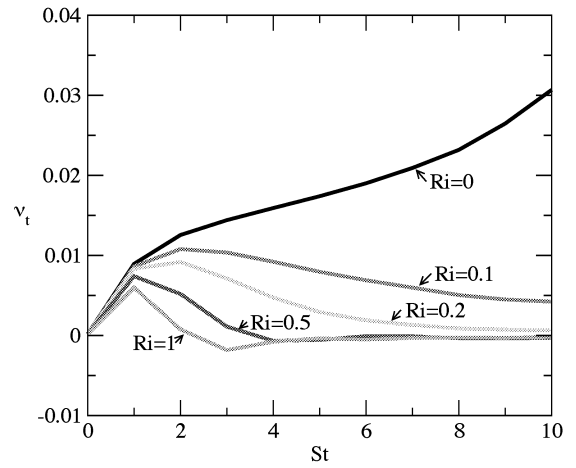


Figure 4: Evolution of the eddy viscosity  $\nu_t$  for a series of simulations in which the Richardson number is varied from  $Ri = 0$  to  $Ri = 1$ . There is no rotation and  $f/S = 0$ .

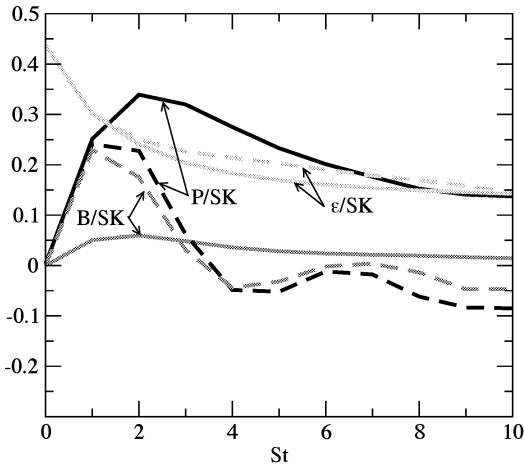


Figure 3: Evolution of the normalized production rate  $P/SK$ , buoyancy flux  $B/SK$ , and dissipation rate  $\epsilon/SK$  for simulations with Richardson numbers  $Ri = 0.1$  (solid lines) and  $Ri = 0.5$  (dashed lines). There is no rotation and  $f/S = 0$ .

8. Rotation decreases the eddy viscosity initially and increases the eddy viscosity later on in the simulations compared to the non-rotating case. The impact increases with increasing ratio  $f/S$ . The eddy viscosity  $\nu_t$  remains positive for all cases and for all times  $St$  throughout the simulations.

Figure 9 shows the final values of  $b_{ij}$  at  $St = 10$  for this series of simulations. As the ratio  $f/S$  is increased, the vertical component  $b_{33}$  increases and for  $f/S = 1$  the components  $b_{22}$  and  $b_{33}$  are approximately equal. The magnitude of the off-diagonal component  $b_{13}$  increases with increasing  $f/S$ . The corresponding turbulence production results in eventual growth of the turbulent kinetic energy in the cases with  $f/S = 0.5$ ,  $f/S = 1$ , and  $f/S = 2$ . The remaining two off-diagonal components  $b_{12}$  and  $b_{23}$  are nonzero in the presence of rotation.

#### Strong Stratification with $Ri = 1$ .

This section repeats the analysis of the previous section

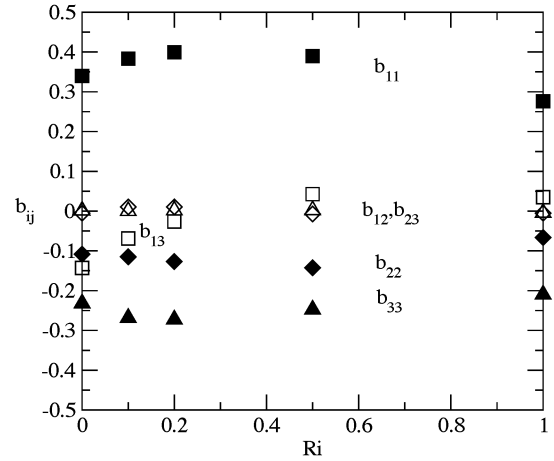


Figure 5: Final values of the shear stress anisotropy  $b_{ij}$  at non-dimensional time  $St = 10$  for a series of simulations in which the Richardson number is varied from  $Ri = 0$  to  $Ri = 1$ . There is no rotation and  $f/S = 0$ .

for strongly stratified flow at a Richardson number  $Ri = 1$ . Figure 10 shows the evolution of the turbulent kinetic energy  $K$ . As the ratio  $f/S$  is increased from  $f/S = 0$  to  $f/S = 2$ , the turbulent kinetic energy shows virtually no effect. Decay of  $K$  is obtained for all cases studied here, including the strongly rotating case with  $f/S = 2$ .

Even a simulation at a more moderate Richardson number  $Ri = 0.3$  and strong rotation  $f/S = 2$  (not shown here) results in a decay of the turbulent kinetic energy, suggesting that the  $Ri > 1/4$  criterion for stability in stratified shear flow derived by Miles (1961) and Howard (1961) holds in the presence of rotation for the range of parameters studied here. This is in contrast to a stability analysis of rotating stably stratified shear flow (Winters and MacKinnon, 2004) that allows for instability at Richardson numbers larger than a quarter.

Figure 11 shows the evolution of the normalized production rate  $P/SK$ , buoyancy flux  $B/SK$ , and  $\epsilon/SK$  for two simulations with  $f/S = 0.1$  and  $f/S = 1$ . Again, only a slight effect of rotation on the normalized dissipation rate  $\epsilon/SK$

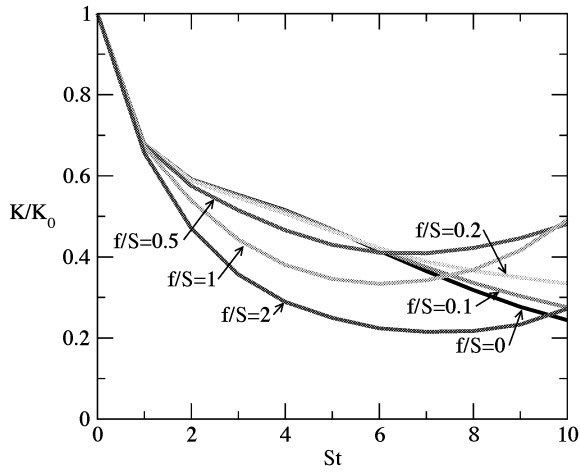


Figure 6: Evolution of the turbulent kinetic energy for a series of simulations in which the ratio  $f/S$  is varied from  $f/S = 0$  to  $f/S = 2$ . The Richardson number  $Ri = 0.2$  is fixed.

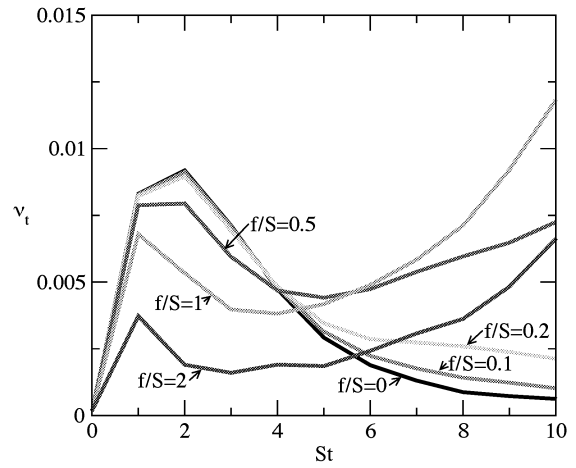


Figure 8: Evolution of the eddy viscosity  $\nu_t$  for a series of simulations in which the ratio  $f/S$  is varied from  $f/S = 0$  to  $f/S = 2$ . The Richardson number  $Ri = 0.2$  is fixed.

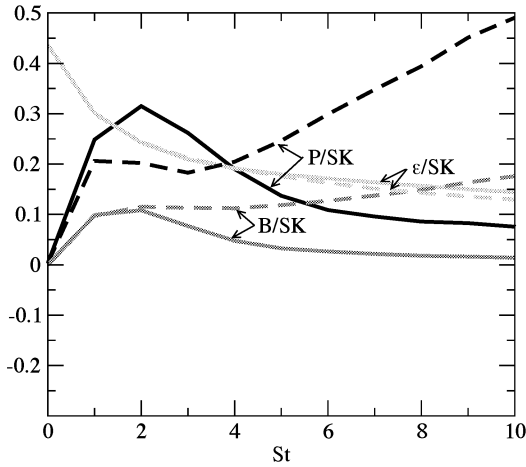


Figure 7: Evolution of the normalized production rate  $P/SK$ , buoyancy flux  $B/SK$ , and dissipation rate  $\epsilon/SK$  for simulations with  $f/S = 0.1$  (solid lines) and  $f/S = 1$  (dashed lines). The Richardson number  $Ri = 0.2$  is fixed.

is observed. Strong rotation does increase the normalized production rate  $P/SK$  and buoyancy flux  $B/SK$  sufficiently to decrease the occurrence of counter-gradient fluxes in this strongly stratified case.

The evolution of the eddy viscosity  $\nu_t$  with non-dimensional time  $St$  is shown in figure 12. Rotation initially affects the values for the eddy viscosity observed in the simulations, again reducing the occurrence of counter-gradient fluxes. In the later evolution of the flow, almost no effect of rotation on the eddy viscosity is obtained.

Figure 13 shows the final values of  $b_{ij}$  at non-dimensional time  $St = 10$ . Almost no impact of a variation of  $f/S$  on the components of  $b_{ij}$  is observed. All off-diagonal components of  $b_{ij}$  remain small in the presence of strong stratification.

## SUMMARY

Direct numerical simulations of the evolution of turbulence in a rotating stably stratified shear flow have been performed.

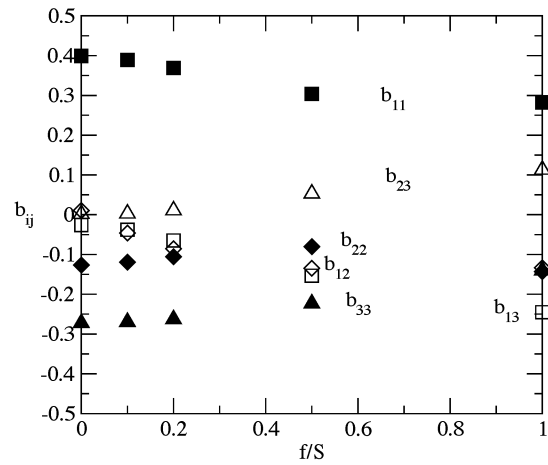


Figure 9: Final values of the shear stress anisotropy  $b_{ij}$  at non-dimensional time  $St = 10$  for a series of simulations in which the ratio  $f/S$  is varied from  $f/S = 0$  to  $f/S = 2$ . The Richardson number  $Ri = 0.2$  is fixed.

The simulations consider rotating stratified shear flow with uniform vertical shear, constant system rotation about the vertical axis, and uniform vertical stable density stratification. A series of non-rotating simulations was performed in which the Richardson number was varied from  $Ri = 0$  to  $Ri = 1$ . As the Richardson number is increased, the growth of the turbulent kinetic energy  $K$  weakens and decay is observed for strongly stratified cases. In the high Richardson number cases, counter-gradient fluxes are observed. Two series of rotating simulations were performed with moderate stratification at a Richardson number of  $Ri = 0.2$  and with strong stratification at a Richardson number  $Ri = 1$ . In both series, the ratio  $f/S$  was varied from  $f/S = 0$  to  $f/S = 2$ . In the  $Ri = 0.2$  series, the evolution of the turbulent kinetic energy changes from decay to growth as the ratio  $f/S$  is increased. Normalized terms in the transport equation for the turbulent kinetic energy are not statistically steady in those cases. In the  $Ri = 1$  series, the evolution of the turbulent kinetic energy shows almost no influence as the ratio  $f/S$  is varied. The fluxes, however, re-

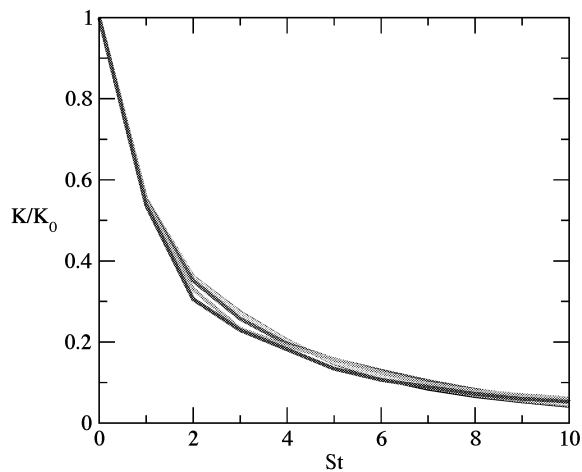


Figure 10: Evolution of the turbulent kinetic energy for a series of simulations in which the ratio  $f/S$  is varied from  $f/S = 0$  to  $f/S = 2$ . The Richardson number  $Ri = 1.0$  is fixed.

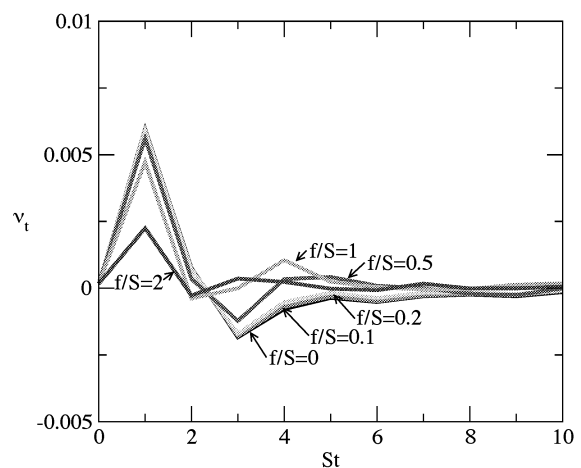


Figure 12: Evolution of the eddy viscosity  $\nu_t$  for a series of simulations in which the ratio  $f/S$  is varied from  $f/S = 0$  to  $f/S = 2$ . The Richardson number  $Ri = 1.0$  is fixed.

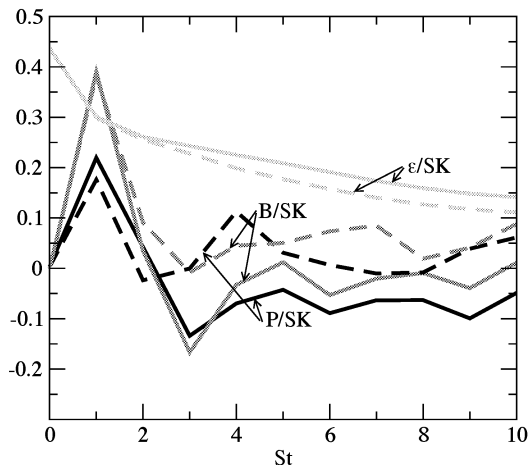


Figure 11: Evolution of the normalized production rate  $P/SK$ , buoyancy flux  $B/SK$ , and dissipation rate  $\epsilon/SK$  for simulations with  $f/S = 0.1$  (solid lines) and  $f/S = 1$  (dashed lines). The Richardson number  $Ri = 1$  is fixed.

mainly mostly down-gradient in the presence of strong rotation. It appears that, for the range of parameters studied here, the  $Ri > 1/4$  criterion for stability in stably stratified shear flow holds in the presence of rotation.

#### ACKNOWLEDGMENTS

I would like to thank the University of San Diego for support of this research project.

#### REFERENCES

Caldwell, D.R., and Moum, J.N., 1995, "Turbulence and mixing in the ocean", *Rev. Geophys.*, Vol. 33, pp. 1385–1394.  
 Gerz, T., Schumann, U., and Elghobashi, S.E., 1989, "Direct numerical simulation of stratified homogeneous turbulent shear flows", *J. Fluid Mech.*, Vol. 200, pp. 563–594.  
 Hanazaki, H., and Hunt, J.C.R., 1996, "Linear Processes in unsteady stably stratified turbulence", *J. Fluid Mech.*, Vol.

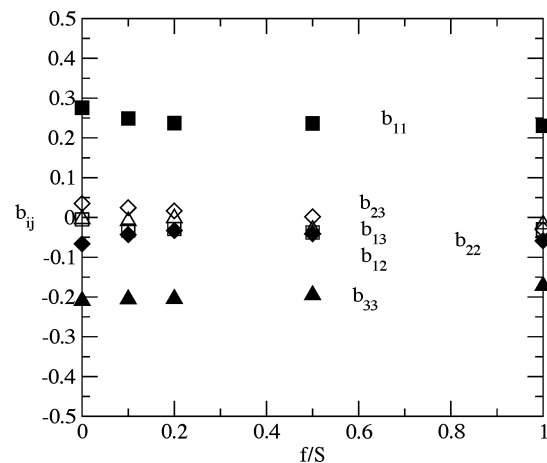


Figure 13: Final values of the shear stress anisotropy  $b_{ij}$  at non-dimensional time  $St = 10$  for a series of simulations in which the ratio  $f/S$  is varied from  $f/S = 0$  to  $f/S = 2$ . The Richardson number  $Ri = 1$  is fixed.

318, pp. 303–337.

Hanazaki, H., 2002, "Linear processes in stably and unstably stratified rotating turbulence", *J. Fluid Mech.*, Vol. 465, pp. 157–190.

Hanazaki, H., and Hunt, J.C.R., 2004, "Structure of unsteady stably stratified turbulence with mean shear", *J. Fluid Mech.*, Vol. 507, pp. 1–42.

Holt, S.E., Koseff, J.R., and Ferziger, J.H., 1992, "A numerical study of the evolution and structure of homogeneous stably stratified sheared turbulence", *J. Fluid Mech.*, Vol. 237, pp. 499–539.

Howard, L.N., 1961, "Note on a paper of John W. Miles", *J. Fluid Mech.*, Vol. 10, 509–512.

Itsweire, E.C., Helland, K.N., and Van Atta, C.W., 1986, "The evolution of grid-generated turbulence in a stably stratified fluid", *J. Fluid Mech.*, Vol. 162, pp. 299–338.

Itsweire, E.C., Koseff, J.R., Briggs, D.A., and Ferziger, J.H., 1993, "Turbulence in stratified shear flows: Implications for interpreting shear-induced mixing in the ocean", *J. Phys.*

*Oceanogr.*, Vol. 23, pp. 1508–1522.

Jacobitz, F.G., Sarkar, S., and Van Atta, C.W., 1997, "Direct numerical simulations of the turbulence evolution in a uniformly sheared and stably stratified flow", *J. Fluid Mech.*, Vol. 342, pp. 231–261.

Jacobitz, F.G., 2000, "Scalar transport and mixing in turbulent stratified shear flow", *Int. J. Heat Fluid Flow*, Vol. 21, pp. 535–541.

Kaltenbach, H.-J., Gerz, T., and Schumann, U., 1994, "Large-eddy simulation of homogeneous turbulence and diffusion in stably stratified shear flow", *J. Fluid Mech.*, Vol. 280, pp. 1–40.

Kimura, Y., and Herring, J.R., 1996, "Diffusion in stably stratified turbulence", *J. Fluid Mech.*, Vol. 328, pp. 253–269.

Komori, S., and Nagata, K., 1986, "Effects of molecular diffusivities on counter-gradient scalar and momentum transfer in strongly stable stratification", *J. Fluid Mech.*, Vol. 326, pp. 205–237.

Komori, S., Ueda, H., Ogino, F., and Mizushima, T., 1983, "Turbulence structure in stably stratified open-channel flow", *J. Fluid Mech.*, Vol. 130, pp. 13–26.

Métais, O., and Herring, J., 1989, "Numerical simulations of freely evolving turbulence in stably stratified fluids", *J. Fluid Mech.*, Vol. 202, pp. 117–148.

Miles, J.W., 1961, "On the stability of heterogeneous shear flows", *J. Fluid Mech.*, Vol. 10, 496–508.

Piccirillo, P.S., and Van Atta, C.W., 1997, "The evolution of a uniformly sheared thermally stratified turbulent flow", *J. Fluid Mech.*, Vol. 334, pp. 61–86.

Richardson, L.F., 1920, "The supply of energy from and to atmospheric eddies", *Proc. Roy. Soc. A*, Vol. 97, 354–373.

Riley, J.J., Metcalfe, R.W., and Weissman, M.A., 1981, "Direct numerical simulations of homogeneous turbulence in density stratified fluids", *Nonlinear Properties of Internal Waves*, AIP Conference Proceedings, Vol. 76, pp. 79–112.

Rogallo, R.S., 1981, "Numerical experiments in homogeneous turbulence", *NASA TM 81315*.

Rohr, J.J., Itsweire, E.C., Helland, K.N., and Van Atta, C.W., 1988, "Growth and decay of turbulence in a stably stratified shear flow", *J. Fluid Mech.*, Vol. 195, pp. 77–111.

Taylor, G.I., 1931, "Effect of variation in density on the stability of superposed streams of fluid", *Proc. Roy. Soc. A*, Vol. 132, 499–523.

Winters, K., and MacKinnon, J., 2004, "The evolution of near-surface inertial motions in the presence of a broad-banded ambient internal wave field", *Eos Trans.*, Vol. 84, Abstract OS41F-05.

Yoon, K., and Warhaft, Z., 1990, "The evolution of grid-generated turbulence under conditions of stable thermal stratification", *J. Fluid Mech.*, Vol. 215, pp. 601–638.